sciendo

POLISH MARITIME RESEARCH 2 (106) 2020 Vol. 27; pp. 85-95
10.2478/pomr-2020-0030

EFFECT OF ENGINE SPEEDS AND DIMETHYL ETHER ON METHYL DECANOATE HCCI COMBUSTION AND EMISSION CHARACTERISTICS BASED ON LOW-SPEED TWO-STROKE DIESEL ENGINE

Shiye Wang
Marine Engineering College, Dalian Maritime University, China
Li Yao
Merchant marine college, Shanghai Maritime University, China

ABSTRACT

The combustion and emission characteristics of homogeneous charge compression ignition (HCCI) fuelled by methyl decanoate (MD) with different engine speeds and dimethyl ether (DME) mixing ratios are investigated in this work. Engine data of a MAN B&W 6S70MC low-speed two-stroke marine diesel engine were used for the reactor. The results show that a decrease of engine speed has little effect on the in-cylinder temperature and pressure of the engine at constant excess air coefficient of 1.5. Meanwhile, NO_x emissions decrease with a decrease of engine speed in pure MD HCCI combustion. The results also indicate that NO_x and CO_2 emissions decrease significantly with an increase in the percentage of DME in MD and DME mixing combustion at a constant total mole fraction and engine speed of 85 revolutions per minute (r/min).

Keywords: Homogeneous charge compression ignition (HCCI),Methyl decanoate (MD),Dimethyl ether (DME),Speed,NOx emission

INTRODUCTION

Nomenclature

HCCI	homogeneous charge compression ignition
MD	methyl decanoate
DME	dimethyl ether
r/min	revolutions per minute
MB	methyl butanoate
VPFR	variable pressure flow reactor
JSR	jet-stirred reactor
NTC	negative temperature coefficient
MH	methyl heptanoate
MO	methyl octanoate
DICI	direct-injection compression-ignition
SI	spark ignition
HTR	high-temperature reaction
CASRN	Chemical Abstracts Service Registry Number
Ar	argon
TS t	ransition states
LTR	low-temperature reaction

It is well known that energy has a significant impact on both the economy and civilization. In future years, energy demands are predicted to increase constantly, especially in developing countries. Conventional diesel, which is derived from fossil fuel, is limited. Due to rapid consumption of fossil fuels, which are the most used source of energy, strong interest in exploring renewable sources and alternative energy solutions to the increasing demand for energy are being vigorously explored.[5][28]

At the same time, the widespread use of fossil fuels as a major source of energy has led to negative societal issues, such as energy security and climate change. The more energy obtained mainly from combustion, the more greenhouse gas, NO_x, and acid rain there are. NO_x, CO, and CO_2 are the important emissions in the engine combustion process. The formation of NO_x is very complex. Harmful NO_x mainly includes NO, NO_2, and N_2O.[3][10][15] To reduce greenhouse gases and NO_x emissions, the emission standards for diesel engines are becoming increasingly stringent. Clean combustion is difficult to achieve in current conditions. Thus,

to reduce dependence on fossil fuels and decrease emissions, clean alternative fuels are becoming increasingly crucial.

Over the past few decades considerable attention have been given to biodiesels, which – although a potentially renewable class of fuels – have similar properties to diesel.[1][14][24] Biodiesels normally come from the transesterification of a lipid (e.g., algal oil, waste oil) with alcohol, resulting in a long-chain mono-alkyl ester.[5] Several excellent advantages of biodiesels for use in diesel engines have been proposed in research studies. On the one hand, these biodiesels have a big advantage over conventional diesel because they are biodegradable, carbon-neutral, non-toxic, and free from sulphur. Biodiesels have lower emissions of particulate matter, CO, CO_2, and unburned hydrocarbons than petrodiesel.[2][11][12][18][20][25][30] On the other hand, in addition to being used as standalone fuels,[38] they can be mixed with petroleum diesel in any proportion. At the same time, they can be used in current diesel engines with small modifications of the engine. Biodiesel is considered as the important fuel of the future; the use of biodiesel will increase quickly. Some countries have drawn up plans to promote biodiesel fuel production and the European Parliament has adopted a series of measures. Emissions of greenhouse gas should have decreased by 25–40% by 2020. By 2050, greenhouse gas should decrease by more than 80%.[6] All European Union member states are actively exploring and vigorously developing the production and use of biodiesel.

Many detailed chemical kinetic mechanisms have been studied to simulate the combustion processes of biodiesels. Methyl butanoate (MB, $C_5H_{10}O_2$), one of the earliest kinetic models, was proposed by Fisher *et al.*[8] as a surrogate of biodiesel. However, the study found that in a variable pressure flow reactor (VPFR) and a jet-stirred reactor (JSR), very little negative temperature coefficient (NTC) behaviour was observed either experimentally or theoretically.[9] Therefore, MB is not suitable as a biodiesel surrogate at low temperatures. A detailed chemical kinetic model of the five major components of rapeseed and soy biodiesel was proposed by Westbrook *et al.*[41] The reaction mechanism consisted of 5,000 species and 20,000 reactions. However, the mechanism is unfeasibly time-consuming and may not be used for flame simulations. Currently, larger methyl esters, such as methyl heptanoate (MH, $C_8H_{16}O_2$) and methyl octanoate (MO, $C_9H_{18}O_2$) have been proposed as surrogates of biodiesels.[4][37] Recently, a chemical kinetic model of methyl decanoate (MD, $C_{11}H_{22}O_2$) was proposed as a surrogate of biodiesels by Herbinet *et al.*[13] The reaction kinetic model of MD is extremely close to actual biodiesel, because both the combustion process and early formation of CO_2 are very similar to conventional diesel.

Dimethyl ether (DME) has a low boiling point and superior auto-ignition ability.[17][33][36][39] Because of its non-toxic and environmentally friendly performance, it does not cause harm to human health. As a new type of alternative fuel, it can be used as an additive to biodiesel with some engine modifications. A DME injector is installed near the inlet port of the cylinder head, as shown by Yao *et al*. The DME injector is controlled by an electromagnetic valve. An electronically controlled fuel injection system allows adjustment of the injected amount of each fuel according to engine operating conditions. A homogeneous mixture of DME and methanol with air was formed during the compression stroke.[42] Low NO_x emissions and almost smoke-free combustion have been proven in the combustion process.[27] At the same time, quite a few research studies have proven that a conventional direct-injection compression-ignition (DICI) engine would obtain high thermal efficiency by using DME.[40]

The HCCI model of internal combustion engines is attracting a lot of attention due to its low NO_x emissions and high efficiency.[19] HCCI combustion includes the strong points of both spark ignition (SI) engines and direct-injection compression-ignition engines. The lean homogeneous fuel/air mixture is essentially inducted into the cylinder without throttling losses. The mixture is compressed to autoignition. These characteristics lead to low NO_x and PM emissions.[22] For these reasons, HCCI has been developed as a low emission mode to replace the traditional diesel combustion system.[34] HCCI ignition largely depends on chemical kinetics. Lots of methods have been used to control ignition and combustion rate.[43] Alternative fuels and fuel mixture can be used to control ignition and the combustion rate, relying on the properties of the engine.[21] Different fuels can be mixed in different proportions to adjust the ignition point at various load–speed areas.[26] Ethers and biodiesel have been applied to HCCI engines.[16][35] Fuel mixture can offer a measure to control HCCI ignition in a wider range than neat fuels.[21] The mixture of n-heptane and isooctane has been used in HCCI engines.[26]

Therefore, the purpose of this research is to decrease NO_x emissions of biodiesel HCCI combustion by mixing with DME. Methods of decreasing NO_x emissions in MD HCCI combustion by decreasing engine speed or mixing with DME in a low-speed two-stroke marine diesel engine are first proposed in this study.

KINETIC MODELS AND METHODS

In this research, a low-speed, two-stroke, in-line, direct-injection marine diesel engine, MAN B&W 6S70MC, was used as the reaction model; the specifications and main parameters of engine are shown in Table 1.[29]

Tab. 1. Test engine specifications

Item	Data
Effective power	13364 kW
Engine speed	85 r/min
Mean effective pressure	15.27 bar
Number of cylinders	6
Stroke	2674 mm
Cylinder diameter	700 mm
Connecting rod length	3066 mm
Scavenging ports opening	39.3° BBDC

Item	Data
Scavenging ports closing	39.3° ABDC
Exhaust valve opening	119° ATDC
Exhaust valve closing	249° ATDC

Simulations of MD, DME, and their mixtures were conducted in the closed internal combustion engine reactor in CHEMKIN-PRO. The chemical reaction mechanism for MD developed by Herbinet *et al*. at the Lawrence Livermore National Laboratory was used as the major reaction mechanism.[13] The mechanism involved 3012 species and 8820 reactions. All the reactions were considered at both low and high temperature reaction stages and the high-temperature reaction (HTR) part of the mechanism was studied as the main reaction process in this work. The DME reaction mechanism model was developed and validated by Fischer *et al.*[7] At the same time, the NO_x reaction mechanism developed by Zeldovich was added as a sub-mechanism.[44] Detailed kinetic and thermodynamic data were included in the mechanism. The properties of MD and DME are given in Table 2.[31]

Tab. 2. Properties of MD and DME

Property	MD	DME
Molecular formula Density (g/cm³ 20°C)	$C_{11}H_{22}O_2$ 0.873	CH_3OCH_3 0.667
Relative molecular weight (kg/kmol)	186	46
Lower heating value (MJ/kg)	34	27.6
Oxygen content (weight %)	17.2	34.8
Flash point (°C)	94	- 42
Boiling point (°C)	224	- 24.5
Cetane number	58.6	60

The MD data came from a search of the Chemical Abstracts Service Registry (CASRN 110-42-9). In order to verify the reliability of the combined mechanism, combustion characteristic curves of DME, DME-NO_x, MD-DME-NOx mechanisms were compared under the same initial conditions. Fig. 1 shows the effect of three reaction mechanisms on in-cylinder temperature and pressure for HCCI combustion. The combined mechanism has little effect on the peak in-cylinder temperature and end temperature at the same initial conditions (Fig. 1(a)). It also has little effect on peak in-cylinder pressure and exhaust pressure (Fig. 1(b)). Therefore, the simulation result indicates that the combined mechanism maintains a high degree of consistency with the original mechanism. For the purpose of achieving complete combustion, the excess air coefficient generally used is 1.4 or 1.5 under normal operating conditions of a two-stroke diesel engine during voyage. The excess air coefficient is set at 1.5 to be consistent with the actual coefficient in this study.

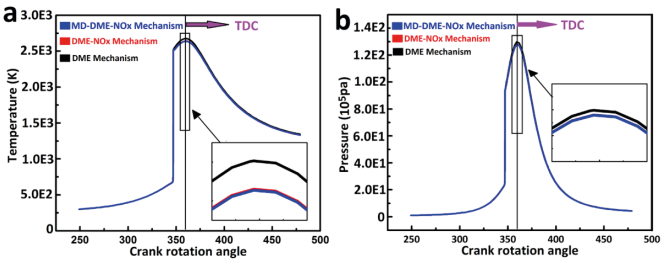

Fig. 1. (a) Effect of combined mechanism on in-cylinder temperature (b) Effect of combined mechanism on in-cylinder pressure

First, at a constant excess air coefficient of 1.5 and the same input fuel energy, combustion of pure MD was carried out in HCCI mode. The combustion and emission processes were simulated with different engine speeds at 85, 75, 65, 55 r/min. Then, at the same engine load, the engine speed was fixed at 85 r/min and the excess air coefficient was fixed at 1.5. DME was mixed with MD in different proportions; the total mole fraction of the mixtures remained unchanged; the composition and cetane number of the same total mole fraction mixtures are given in Table 3. To ensure the total mole fraction remained unchanged, argon (Ar) was used as the shielding gas or filling gas which did not participate in the reaction in the combustion process.

Tab. 3. Composition and cetane number of the same total mole fraction mixtures

Mole fraction of MD	Mole fraction of DME	Mole fraction of O_2	Mole fraction of N_2	Mole fraction of Ar	Cetane number
1.0	0	23.25	87.46	0	58.60
0.8	0.2	19.50	73.36	17.85	58.88
0.6	0.4	15.75	59.25	35.71	59.16
0.4	0.6	12.0	45.14	53.57	59.44
0.2	0.8	8.25	31.04	71.42	59.72

RESULTS AND DISCUSSION

The first section of this paper deals with the effects of decreasing engine speed on MD HCCI combustion. Then, this study shows the combustion and emission characteristics of mixtures with different mixing ratios of MD and DME.

EFFECT OF DECREASING ENGINE SPEED ON MD HCCI COMBUSTION AND EMISSION CHARACTERISTICS

In-Cylinder Temperature and Pressure at Different Speeds

In-cylinder temperature and pressure have important effects in the engine combustion process. Fig. 2 shows the effect of decreasing engine speed on in-cylinder temperature and pressure of MD HCCI combustion. A decrease of engine speed from 85 to 55 r/min has little effect on the peak in-cylinder temperature and end temperature at a constant MD mole fraction (Fig. 2(a)). It also has little effect on the peak in-cylinder pressure and exhaust pressure at a constant MD mole fraction (Fig. 2(b)). Therefore, the simulation result indicates that a decrease of engine speed has little effect on

in-cylinder temperature and pressure; that is to say, a decrease of engine speed does not affect the efficiency of the engine.

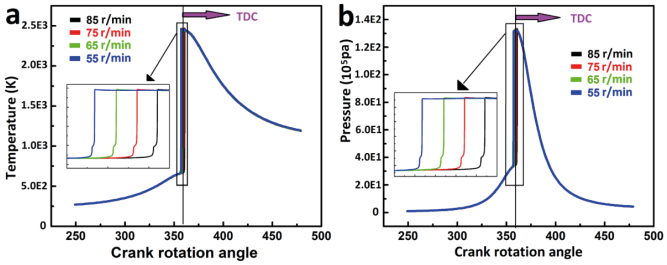

Fig. 2. (a) Effect of decreasing engine speed on in-cylinder temperature (b) Effect of decreasing engine speed on in-cylinder pressure

The experimental results of cylinder pressure change in a marine diesel engine are shown in Fig. 3. The trend of changing pressure in the theoretical calculation agreed with the actual data from the YU KUN ship. Combustion pressure data were derived from an operational ship's main engine and recorded by its monitoring system. The compression medium of the HCCI cycle is homogeneous premixed gas. It is assumed that when the temperature reaches the ignition point, the fuel is burned completely. Because the combustion model is ideal, when the temperature reaches the ignition point, the combustion process is completed immediately and the in-cylinder pressure rises abruptly. Combustion in a diesel cycle is gradual and only when reaction conditions are formed in turn can the fuel be burned completely. The combustion process needs some time; thus, the combustion reaction rate accelerates gradually and the in-cylinder pressure increases gradually. When compared with Fig. 2(b), it can be seen that HCCI theoretical calculations of peak in-cylinder and exhaust pressure maintain a positive consistency with the diesel experimental data. Therefore, the reliability of this simulation calculation is guaranteed.

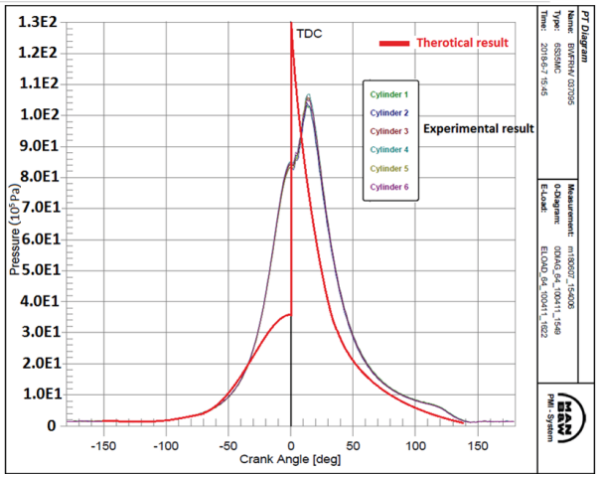

Fig. 3. Cylinder pressure of marine diesel engine

NO_x Emissions at Different Speeds

Fig. 4 illustrates the relationship between NO_x emissions and engine speed in MD HCCI combustion. The NO_x emissions at different engine speeds are shown by different coloured lines. When the constant excess air coefficient is 1.5, NO emissions decrease with a decrease in engine speed from 85 to 55 r/min (Fig. 4(a)). This trend is similar to that of NO emissions. The amount of NO_2 emissions in HCCI combustion becomes less with a decrease of engine speed from 85 to 55 r/min, as shown in Fig. 4(b). Fig. 4(c) shows that a decrease of engine speed from 85 to 55 r/min has little effect on N_2O emissions. A decrease of engine speed causes the perturbation of gas in the cylinder to weaken and the flame propagation speed to slow down. Thermal NO_x is the main type of NO_x emission in the engine combustion process. Temperature, oxygen content, and reaction time are major factors of thermal NO_x formation. At a constant excess air coefficient of 1.5 the amount of fuel remains the same, so the oxygen content is unchanged. A decrease of engine speed from 85 to 55 r/min has little effect on the peak in-cylinder temperature and end temperature. Reaction time is prolonged with a decrease in engine speed. There is more reaction time for the destruction of NO_x in the combustion process at a lower engine speed which eventually results in lower NO_x. It can be concluded that the amount of NO_x emissions in MD HCCI combustion becomes less with a decrease in engine speed. That is to say, low NO_x emissions could be obtained by decreasing engine speed appropriately. The simulation result indicates that the most NO_x is produced during the HTR, and it is obvious that the main reaction process of NO_x occurs at a crank rotation angle range of 355° to 400°, as shown in Fig. 4.

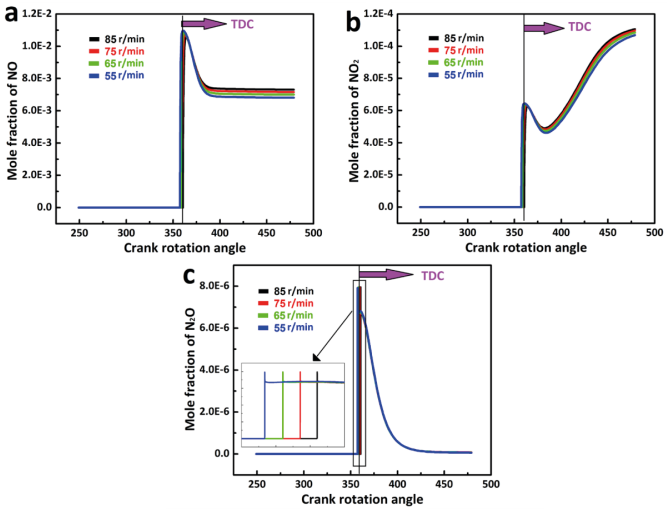

Fig. 4. (a) Effect of decreasing engine speed on NO emissions (b) Effect of decreasing engine speed on NO_2 emissions (c) Effect of decreasing engine speed on N_2O emissions

Fig. 5 shows that in the main reaction process (crank rotation angle range of 355° to 400°) of MD combustion, the reaction path diagram of the greatest NO_x mole fraction is produced with an engine speed of 85 r/min. The width of the arrow provides an intuitionistic optical indication of reaction rates of the NO_x reaction path. The absolute rate of the greatest NO, NO_2, N_2O mole fractions produced are shown in Fig. 5.

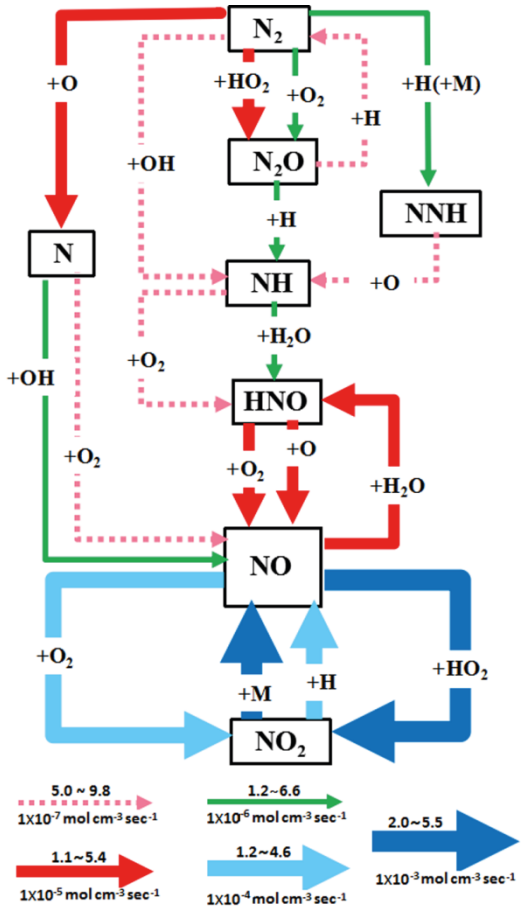

Fig. 5. Reaction path of NO_x emissions for MD HCCI combustion

In an attempt to understand the reaction process of NO_x intuitively, transition states (TS) for the main reaction of NO_x are given. Important reactions of NO_x are extracted to analyse the reaction path in the study. The anharmonic effect is added to the reactant and transition states for high accuracy calculation. Calculation of the reaction channel and transition state were completed by the research group.[45] The calculated results of the rate constants were compared with the experimental data to observe the effect of adding anharmonic effect to the rate constant. The anharmonic effect cannot be ignored when the differences between the calculated results and the experimental data are large; however, small differences indicate that the anharmonic effect can be ignored. It is obvious that the production of NO comes mainly from the reaction of NO_2. Fig. 6(a) shows energy and geometries of reactant, transition state, and products for the reaction P1. The reaction P1 has one reaction channel and one transition state. The ball-and-stick models of Channel 1 show that the oxygen atom approaches NO gradually and combines with NO to eventually produce NO_2. The energy and geometries of the reactant, transition state, and products for reaction P2 are shown in Fig. 6(b). The reaction P2 has three reaction channels and seven transition states. Channel 2 shows that the hydrogen atom approaches NO_2 and combines with a nitrogen atom. Then, the hydrogen atom detaches from the nitrogen atom and combines with an oxygen atom detached from NO_2 to produce NO and OH. Channel 3 and Channel 4 show that the hydrogen atom approaches NO_2 and combines with an oxygen atom detached from NO_2 to produce NO and OH.

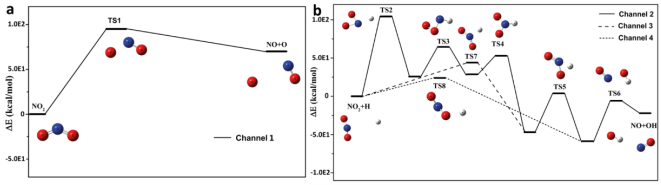

Fig. 6. (a) The optimized energy and geometries of reactant, transition state, and products for reaction P1 (b) The optimized energy and geometries of reactant, transition state, and products for reaction P2

The major reactions are shown according to the following chemical equations:

$$\text{Channel1: } NO_2 + M \xrightarrow{TS1} NO + O + M \qquad \textbf{(P1)}$$

$$\text{Channel2: } NO_2 + H \xrightarrow{TS2\rightarrow TS3\rightarrow TS4\rightarrow TS5\rightarrow TS6} NO + OH$$

$$\text{Channel3: } NO_2 + H \xrightarrow{TS7\rightarrow TS5\rightarrow TS6} NO + OH \qquad \textbf{(P2)}$$

$$\text{Channel4: } NO_2 + H \xrightarrow{TS8\rightarrow TS5\rightarrow TS6} NO + OH$$

The production of NO_2 comes mainly from the reaction of NO. Fig. 7(a) shows energy and geometries of reactant, transition state, and products for reaction P3. The reaction P3 has one reaction channel and one transition state. The ball-and-stick models show that the oxygen atom on HO_2 approaches NO gradually, becomes detached from HO_2, and combines with NO to eventually produce NO_2. The energy and geometries of reactant, transition state, and products for reaction P4 are shown in Fig. 7(b). The reaction P4 has one reaction channel and one transition state. It shows that O_2 approaches NO gradually, and one oxygen atom becomes detached from O_2 and combines with NO to produce NO_2 and O.

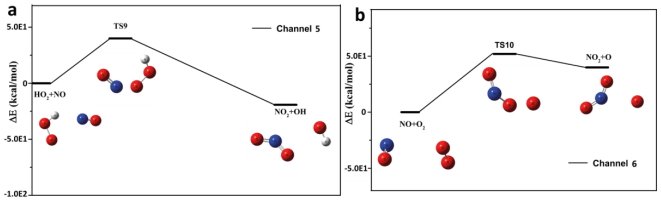

Fig. 7. (a) The optimized energy and geometries of reactant, transition state, and products for reaction P3 (b) The optimized energy and geometries of reactant, transition state, and products for reaction P4

The major reactions are shown according to the following chemical equations:

$$\text{Channel5: } NO + HO_2 \xrightarrow{TS9} NO_2 + OH \quad \textbf{(P3)}$$

$$\text{Channel6: } NO + O_2 \xrightarrow{TS10} NO_2 + O \quad \textbf{(P4)}$$

The production of N_2O comes mainly from the reaction of N_2; Fig. 8(a) shows energy and geometries of reactant, transition state, and products for reaction P5. The reaction P5 has one reaction channel and one transition state. It shows that one oxygen atom becomes detached from HO_2 and combines with N_2 to eventually produce N_2O and OH. The energy and geometries of reactant, transition state, and products for reaction P6 are shown in Fig. 8(b). The reaction P6 has one reaction channel and one transition state. It shows that N_2 approaches O_2 gradually, and one oxygen atom becomes detached from O_2 and combines with N_2 to eventually produce N_2O and O.

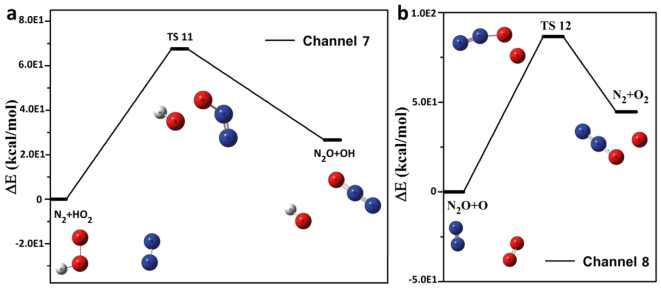

Fig. 8. (a) The optimized energy and geometries of reactant, transition state, and products for reaction P5 (b) The optimized energy and geometries of reactant, transition state, and products for reaction P6

The major reactions are shown according to the following chemical equations:

$$\text{Channel7: } N_2 + HO_2 \xrightarrow{TS11} N_2O + OH \quad \textbf{(P5)}$$

$$\text{Channel8: } N_2 + O_2 \xrightarrow{TS12} N_2O + O \quad \textbf{(P6)}$$

CO and CO_2 Emissions at Different Speeds

CO and CO_2 are major emissions of the combustion process. Fig. 9 shows the effect of decreasing engine speed on CO and CO_2 emissions in MD HCCI combustion. Fig. 9(a) shows that at a constant excess air coefficient 1.5, a decrease of engine speed from 85 to 55 r/min has little effect on CO emissions. Production of CO_2 emissions has changed only by a small amount with a decrease of engine speed at a constant fuel–air ratio, as shown in Fig. 9(b). HCCI combustion of MD is completed at an excess air coefficient of 1.5; that is to say, carbon will burn completely to become CO_2. A decrease of engine speed from 85 to 55 r/min has little effect on peak in-cylinder temperature and end temperature in Fig. 2(a). Thus, speed reduction will not result in poor combustion. Carbon is burned completely to become CO and CO_2; then, CO is burned completely and finally oxidized to CO_2. Because the complete combustion of carbon is not affected by a decrease of speed, the emissions of CO and CO_2 remain almost unchanged. Therefore, the simulation result indicates that a decrease in engine speed has little effect on CO and CO_2 emissions.

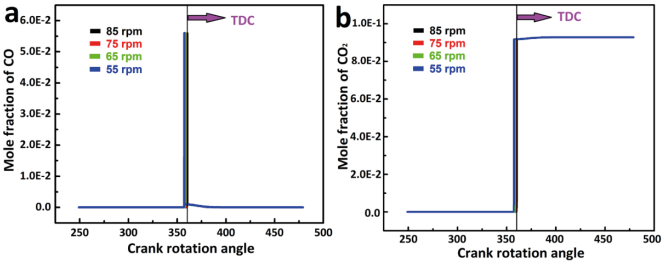

Fig. 9. (a) Effect of decreasing engine speed on CO emissions. (b) Effect of decreasing engine speed on CO_2 emissions.

COMBUSTION AND EMISSION CHARACTERISTICS OF THE SAME TOTAL MOLE FRACTION MIXTURES WITH DIFFERENT MD AND DME BLENDING RATIOS

Effect of MD and DME Mixing Ratio on In-Cylinder Temperature and Pressure

Fig. 10 shows, at an engine speed of 85 r/min, the profiles of in-cylinder combustion temperature and pressure during the HCCI combustion process for mixtures with different mixing ratios of MD and DME. Fig. 10(a) shows that the end temperature and maximum combustion temperature in-cylinder decrease with an increase of DME percentage at a constant engine speed of 85 r/min, which is because the DME has the lower heating value than MD(Table 2). The relative molecular weight of MD is much larger than the DME. At a constant total mole fraction, the total heating value reduces with an increase of DME percentage. Therefore, the temperature can be regulated in a suitable range by adjusting the mixing ratios of MD and DME. A decrease in the peak combustion temperature in the cylinder has an inhibitory effect on the formation of NO_x.[23][32] The cetane number of dimethyl ether is higher than that of methyl decanoate (Table 2), so the self-ignition combustion temperature of DME is lower than that of MD. As the DME mixture ratio increases, the cetane number of the mixed fuel increases (Table 3), while the self-ignition combustion temperature of the mixed fuel is reduced. As a result, the ignition delay time is shortened, and combustion efficiency is improved. At the same time, a decrease of end temperature can effectively reduce vibration and extend engine part life. The effect of DME percentage on in-cylinder pressure is shown in Fig. 10(b). It can be observed that the peak in-cylinder pressure undergoes a small decrease with an increase in the DME blending ratio, and the decrease of peak in-cylinder pressure can reduce the frequency of knocking. Therefore, the simulation result indicates that the percentage of MD and DME is an important factor that influences HCCI combustion. For the purpose of optimizing the combustion process, it is indispensable to adjust an appropriate mixing ratio of MD and DME.

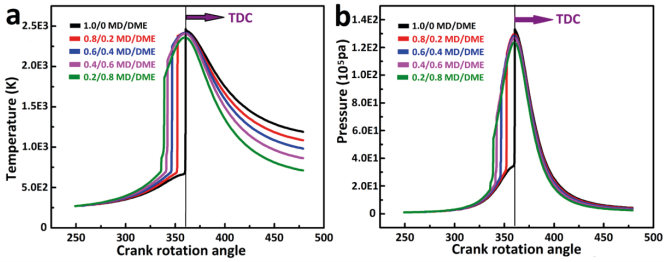

Fig. 10. (a) Effect of DME percentage on in-cylinder temperature (b) Effect of DME percentage on in-cylinder pressure

Effect of MD and DME Mixing Ratio on NO_x Emissions

Fig. 11 shows, at a constant total mole fraction, the effect of MD and DME mixing ratio on NO_x emissions. The amount of NO emissions is reduced significantly with an increase of DME percentage at the different proportion of mixtures (Fig. 11(a)). The trend is similar to that of NO emissions: with a rise of DME mixing ratio, NO_2 emissions decrease significantly at a constant total mole fraction, as shown in Fig. 11(b). Fig. 11(c) shows that the maximum production of N_2O decreases with an increase of the DME mixing ratio. The formation of NO_x is related to the combustion temperature: the peak combustion temperature decreases with an increase of DME percentage. Thus, NO emissions are reduced with decreases in combustion temperature.[23][32]

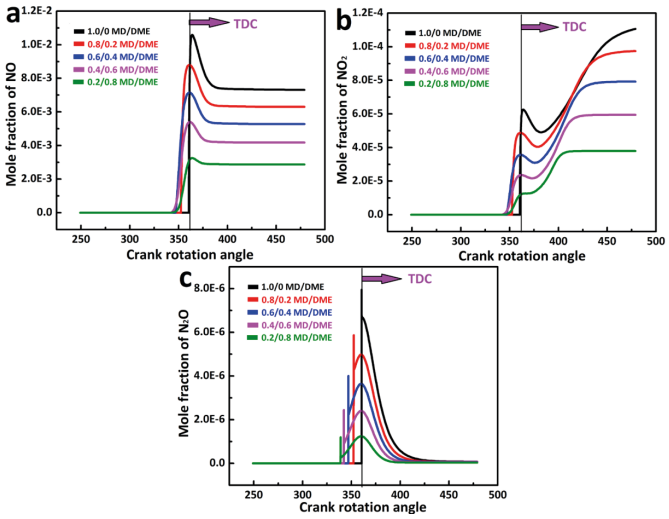

Fig. 11.
(a) Effect of DME percentage on NO emissions at a constant mole fraction
(b) Effect of DME percentage on NO_2 emissions at a constant mole fraction
(c) Effect of DME percentage on N_2O emissions at a constant mole fraction

Effect of MD and DME Mixing Ratio on NO_x Reaction Rate

Fig. 12 shows the effect of MD and DME blending ratio on NO reaction rate in the main reaction process which is mentioned above. It clearly indicates that the combustion reaction rate of NO is reduced with a rise of DME percentage, and the reason for the reduction of the NO reaction rate is due to a decrease of combustion temperature. The low temperature weakens the perturbation of gas in-cylinder; thus, the reaction rate of NO reduces, which leads to a decrease in NO emissions.

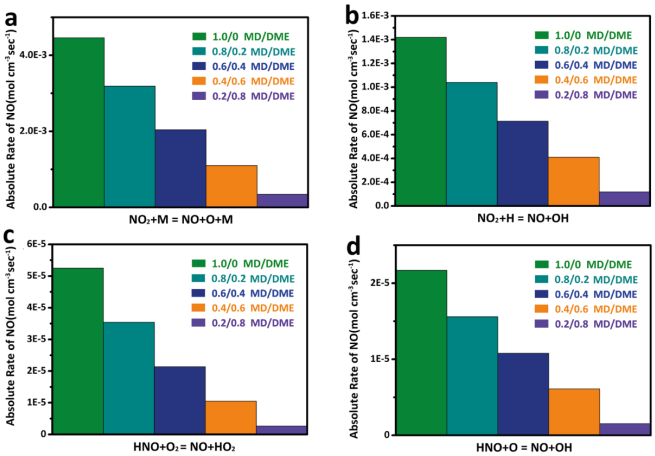

Fig. 12. Effect of MD and DME mixing ratio on NO reaction rate at a constant mole fraction

The effect of MD and DME mixing ratio on NO_2 reaction rate in the main reaction process at a constant total mole fraction is shown in Fig. 13. With the rise of DME percentage, the reaction rate of NO_2 decreases due to the decrease of combustion temperature, which leads to a decrease of NO_2 emissions.

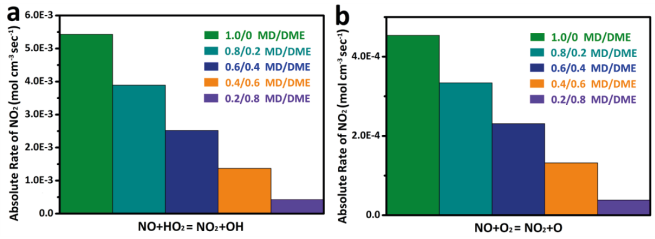

Fig. 13. Effect of MD and DME mixing ration on NO_2 reaction rate at a constant mole fraction.

The trend is similar to that of the NO and NO_2 reaction rate: the reaction rate of N_2O decreases with an increase of DME mixing ratio in the main reaction process (Fig. 14). A high DME percentage leads to a low combustion temperature; thus, the reaction rate of N_2O decreases, which means low NO_2 emissions.

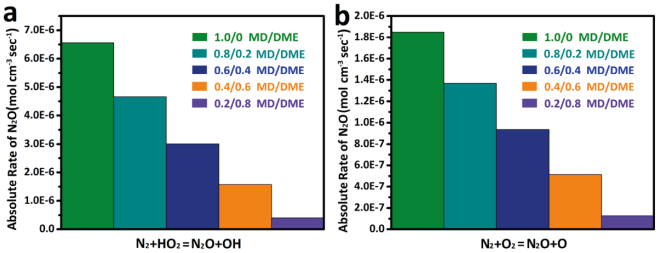

Fig. 14. Effect of MD and DME mixing ratio on N_2O reaction rate at a constant mole fraction

Therefore, it is clear that the reaction rate of NO_x decreases significantly with an increase of DME mixing ratio at a constant total mole fraction. That is to say, NO_x emissions can be decreased by increasing DME percentage in a suitable range.

Effect of MD and DME Mixing Ratio on CO and CO_2 Emissions

Fig. 15 shows the effect of MD and DME mixing ratio on CO and CO_2 emissions at a constant total mole fraction. The maximum production of CO decreases with an increase of DME mixing ratio, as shown in Fig. 15(a). Fig. 15(b) shows that the amount of CO_2 emissions decreases significantly with an increase of DME percentage. The reason for the reduction of CO_2 emissions is that the DME has lower C/H ratio relative to MD; an increase of DME mixing ratio can decrease the C/H ratio of the mixture and reduce CO_2 emissions effectively. Therefore, it can be concluded that the amount of CO_2 emissions in HCCI combustion becomes less with an increase of DME mixing ratio.

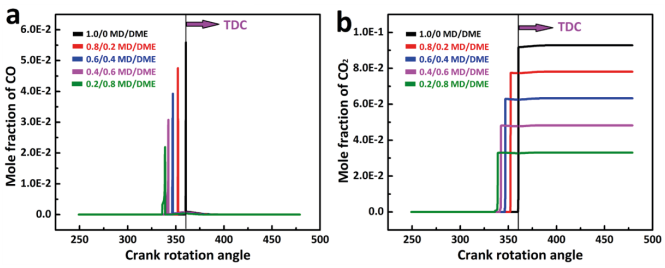

Fig. 15. (a) Effect of DME percentage on CO emissions at a constant mole fraction (b) Effect of DME percentage on CO_2 emissions at a constant mole fraction

Effect of MD and DME Mixing Ratio on Heat Release Rates

At a constant total mole fraction and engine speed of 85 r/min, the heat release rate curves of MD and DME mixed at different mixing ratios are given in Fig. 16. There are two peak values in the curve of each mixture. The higher peak value appears in HTR; the other appears in low-temperature reaction (LTR). The releasing heat of HTR takes up to above 95% of the total combustion process. Because the relative molecular weight of MD is much larger than DME, at a constant total mole fraction, heat release rates decrease with an increase of DME percentage. At a constant total heating value, the peak values of the mixture heat release rate curve have small distinctions. However, the amount of NO and NO_2 emissions changes very little, so there is no significance when comparing the heat release rate curves.

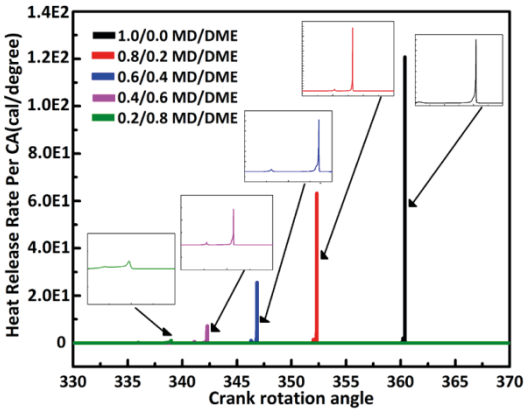

Fig. 16. Heat release rate of MD and DME mix with different mixing ratios

CONCLUSIONS

A skeletal mechanism was completed by combining an MD mechanism, DME mechanism, and NO_x mechanism. Through sensitivity analysis, changes of combustion temperature, pressure, and NO_x, CO, and CO_2 emissions during the combustion of methyl decanoate HCCI were obtained for different engine speeds and different DME mixture ratios. The main chemical reaction paths and chemical reaction rates of NO, NO_2, and N_2O could be observed accurately by analysis of the reaction path.

NO_x emissions of MD HCCI combustion decrease with a decrease of engine speed from 85 to 55 r/min on low-speed two-stroke marine diesel engines. Therefore, NO_x emissions can be reduced by adjusting diesel engine speed in a suitable range. The decrease of engine speed from 85 to 55 r/min has little effect on CO and CO_2 emissions of MD HCCI combustion. Therefore, a decrease of engine speed does not cause a rise of CO and CO_2 emissions at the same input fuel energy.

Different MD and DME mixing ratios were used at the same total mole fraction and, with an increase of DME ratio, the exhaust temperature and in-cylinder peak temperature decreased, the cetane number of the mixed fuel increased, ignition delay time was shortened, and combustion efficiency improved. The amount of NO_x emissions decreased significantly with an increase of DME mixing ratio. The absolute reaction rate of NO_x decreased significantly with an increase of the DME mixing ratio in the main reaction process. NO_x emissions decreased due to a decrease of reaction rate. Therefore, NO_x emissions of MD HCCI combustion can be reduced by DME addition in low-speed two-stroke marine diesel engines. At the same time, CO_2 emissions experience a certain decline with an increase in DME percentage. CO_2 emissions of MD HCCI combustion can be reduced by DME addition in low-speed two-stroke marine diesel engines. Therefore, the combustion and emission process of MD HCCI combustion can be optimized by increasing the percentage of DME at the same engine load.

ACKNOWLEDGMENTS

The project was supported by the Major Research Plan of the National Natural Science Foundation of China (91441132). Research on Intelligent Ship Testing and Verification.

REFERENCES

1. Ashraful, A. M., Masjuki, H. H., Kalam, M. A., Rizwanul Fattah, I. M., Imtenan, S., Shahir, S. A., Mobarak, H. M. (2014) *Production and Comparison of Fuel Properties, Engine Performance, and Emission Characteristics of Biodiesel from Various Non–Edible Vegetable Oils: A Review.* Energy Convers. Manage., Vol. 80, 202–228.

2. Buyukkaya, E. (2010) *Effects of Biodiesel on A DI Diesel Engine Performance, Emission and Combustion Characteristics.* Fuel, Vol. 89(10), 3099–3105.

3. Cho, C. P., Pyo, Y. D., Jang, J. Y., Kim, G. C., Shin, Y. J. (2017) *NO_x Reduction and N_2O Emissions in A Diesel Engine Exhaust Using Fe–Zeolite and Vanadium based SCR Catalysts.* Appl. Therm. Eng., Vol. 110, 18–24.

4. Dayma, G., Togbé, C., Dagaut, P. (2009) *Detailed Kinetic Mechanism for the Oxidation of Vegetable Oil Methyl Esters: New Evidence from Methyl Heptanoate.* Energy Fuels, Vol. 23(9), 4254–4268.

5. Demirbas, A. (2007) *Importance of Biodiesel as Transportation Fuel.* Energy Policy, Vol. 35(9), 4661–4670.

6. European Parliament, *2050, The Future Begins Today-Recommendations for the EU's Future Integrated Policy on Climate Change*.

7. Fischer, S. L., F. L. Dryer., Curran, H. J. (2000) *The Reaction Kinetics of Dimethyl Ether. I: High–Temperature Pyrolysis and Oxidation in Flow Reactors.* Int. J. Chem. Kinet., Vol. 32(12), 713–740.

8. Fisher, E. M., Pitz, W. J., Curran, H. J., Westbrook, C. K. (2000) *Detailed Chemical Kinetic Mechanisms for Combustion of Oxygenated Fuel.* Proc. Combust. Inst., Vol. 28(2), 1579–1586.

9. Gaïl, S., Thomson, M. J., Sarathy, S. M., Syed, S. A., Dagaut, P., Dievart, P., Marchese, A. J., Dryer, F. L. (2007) *A Wide–Ranging Kinetic Modeling Study of Methyl Butanoate Combustion.* Proc. Combust. Inst., Vol. 31 (1), 305–311.

10. Geng, P., Tan, Q. M., Zhang, C. H., Wei, L. J., He, X. Z., Cao, E. M., Jiang, K. (2016) *Experimental Investigation on NO_x and Green House Gas Emissions from A Marine Auxiliary Diesel Engine Using Ultralow Sulfur Light Fuel.* Sci. Total Environ., Vol. 572, 467–475.

11. He, C., Ge, Y. S., Tan, J. W., You, K. W., Han, X. K., Wang, J. F. (2010) *Characteristics of Polycyclic Aromatic Hydrocarbons Emissions of Diesel Engine Fueled with Biodiesel and Diesel.* Fuel, Vol. 89(8), 2040–2046.

12. Haas, M. J., Scott, K. M., Alleman, T. L., McCormick, R. L. (2001) *Engine Performance of Biodiesel Fuel Prepared from Soybean Soapstock: A High Quality Renewable Fuel Produced from A Waste Feedstock*. Energy Fuels, Vol. 15(5), 1207–1212.

13. Herbinet, O., Pitz, W. J., Westbrook, C. K. (2008) *Detailed Chemical Kinetic Oxidation Mechanism for a Biodiesel Surrogate*. Combust. Flame, Vol. 154(3), 507–528.

14. Hou, J., Zhang, P., Yuan, X., Zheng, Y. (2011) *Life Cycle Assessment of Biodiesel from Soybean, Jatropha and Microalgae in China Conditions*. Renew. Sust. Energ Rev., Vol. 15(9), 5081–5091.

15. Jeon, J., Lee, J. T., Park, S. (2016) *Nitrogen Compounds (NO, NO_2, N_2O and NH_3) in NO_x Emissions from Commercial EURO VI Type Heavy–Duty Diesel Engines with A Urea–Selective Catalytic Reduction System.* Energy Fuels, Vol. 30(8), 6828–6834.

16. Jothi, N. K. M., Nagarajan, G., Renganarayanan, S. (2007) *Experimental Studies on Homogeneous Charge CI Engine Fueled with LPG Using DEE as An Ignition Enhancer.* Renew Energ., Vol. 32(9), 1581–1593.

17. Kim, M. Y., Yoon, S. H., Ryu, B. W., Lee, C. S. (2008) *Combustion and Emission Characteristics of DME as An Alternative Fuel for Compression Ignitions with A High Pressure Injection System.* Fuel, Vol. 87(12), 2779– 2786.

18. Koshe-Höinghaus, K., Oßwald, P., Cool, T., Kasper, T., Hansen, N., Qi, F., Westbrook, C. K., Westmoreland, P. R. (2010) *Biofuel Combustion Chemistry: From Ethanol to Biodiesel.* Angew. Chem. Int., Vol. 49(21), 3572–3597.

19. Kumar, P., Rehman, A. (2016) *Bio-Diesel in Homogeneous Charge Compression Ignition (HCCI) Combustion.* Renew. Sust. Energ. Rev., Vol. 56, 536–550.

20. Lai, J. Y. W., Lin, K. C., Violi, A. (2011) *Biodiesel Combustion: Advances in Chemical Kinetic Modeling.* Prog. Energy Combust. Sci., Vol. 37(1), 1–14.

21. Lu, X. C., Han, D. Huang, Z. (2011) *Fuel Design and Management for the Control of Advanced Compression-ignition Combustion Modes.* Prog. Energ. Combust., Vol. 37(6), 741–783.

22. Ma, J. J., Lue, X. C., Ji, L. B. (2008) *An Experimental Study of HCCI-DI Combustion and Emissions in A Diesel Engine with Dual Fuel.* Int. J. Therm. Sci., Vol. 47(9), 1235–1242.

23. Miller, J., Bowman, C. (1989) *Mechanism and Modeling of Nitrogen Chemistry in Combustion*. Prog. Energy Combust. Sci., Vol. 15(4), 287–338.

24. Moradi, G. R., Dehghani, S., Ghanei, R. (2012) *Measurements of Physical Properties During Transesterification of Soybean Oil to Biodiesel for Prediction of Reaction Progress.* Energy Convers. Manage., Vol. 61, 67–70.

25. Ng, J. H., Ng, H. K., Gan, S. Y. (2012) *Characterisation of Engine–Out Responses from A Light-Duty Diesel Engine Fuelled with Palm Methyl Ester (PME).* Appl. Energ., Vol. 90(1), 58–67.

26. Olsson, J. O., Tunestal, P., Johansson, B. (2001) Closed-Loop Control of An HCCI Engine. SAE, Vol. 110, 1076–1185.

27. Park, S. H., Lee, C. S. (2014) *Applicability of Dimethyl Ether (DME) in A Compression Ignition Engine as An Alternative Fuel.* Energy Convers. Manage., Vol. 86, 848–863.

28. Pienkos, P. T., Darzins, A. (2009) *The Promise and Challenges of Microalgal–Derived Biofuels.* Biofuels Bioprod Bioref., Vol. 3(4), 431–440.

29. Radica, G., Antonić, R., Račić, N. (2009) *Engine Working Cycle Analysis for Diagnostic and Optimisation Purposes.* Brodogradnja, Vol. 60(4), 378–387.

30. Rajasekar, E., Murugesan, A., Subramanian, R., Nedunchezhian, N. (2010) *Review of NO_x Reduction Technologies in CI Engines Fuelled with Oxygenated Biomass Fuels.* Renew. Sust Energ Rev., Vol. 14(7), 2113–2121.

31. Roh, H. Gu., Lee, D., Lee, C. S. (2015) *Impact of DME-Biodiesel, Diesel-Biodiesel and Diesel Fuels on the Combustion and Emission Reduction Characteristics of A CI Engine According to Pilot and Single Injection Strategies.* J. Energy Inst., Vol. 88(4), 376–385.

32. Santner, J., Ahmed, S. F., Farouk, T., Dryer, F. L. (2016) *Computational Study of NO_x Formation at Conditions Relevant to Gas Turbine Operation: Part 1.* Energy Fuels, Vol. 30(8), 6745–6755.

33. Semelsberger, T. A., Borup, R. L., Howard, L., Greene, H. L. (2006) *Dimethyl Ether (DME) as An Alternative Fuel.* J. Power Sources, Vol. 156(2), 497–511.

34. Sjoberg, M., Dec, J. E. (2005) *An Investigation into Lowest Acceptable Combustion Temperatures for Hydrocarbon Fuels in HCCI Engines.* P. Combust. Inst., Vol. 30, 2719–2726.

35. Szybist, J. P., Mcfarlane, J., Bunting, B. G. (2007) *Comparison of Simulated and Experimental Combustion of Biodiesel Blends in A Single Cylinder Diesel HCCI Engine.* SAE.

36. Thomas, G., Feng, B., Veeraragvan, A., Cleary, M. J., Drinnan, N. (2014) *Emissions from DME Combustion in Diesel Engines and Their Implications on Meeting Future Emission Norms: A Review.* Fuel Process Technol., Vol. 119, 286–304.

37. Togbé, C., May-Carle, J-B., Dayma, G., Dagaut, P. (2010) *Chemical Kinetic Study of the Oxidation of A Biodiesel–Bioethanol Surrogate Fuel: Methyl Octanoate–Ethanol Mixtures.* J. Phys. Chem. A, Vol. 114(11), 3896–3908.

38. Tyson, K. S. (2001) Biodiesel Handling and Use Guidelines, National Renewable Energy Laboratory (NREL): Golden, CO, NREL/TP-580-30004.

39. Wang, Y., Zhao, Y., Yang, Z. (2013) *Dimethyl Ether Energy Ratio Effects in A Dimethyl Ether-Diesel Dual Fuel Premixed Charge Compression Ignition Engine.* Applied Thermal Engineering, Vol. 54(2), 481–487.

40. Wang, Y., Zhou, L. B., Yang, Z. J., Dong, H. Y. (2005) *Study on Combustion and Emission Characteristics of a Vehicle Engine Fuelled with Dimethyl Ether.* Proc. Inst. Mech. Eng. Part D J. Automob. Eng., Vol. 219(2), 263–269.

41. Westbrook, C. K., Naik, C. V., Herbinet, O., Pitz, W. J., Mehl, M., Sarathy, S.M. et al. (2011) *Detailed Chemical Kinetic Reaction Mechanisms for Soy and Rapeseed Biodiesel Fuels.* Combust. Flame, Vol. 158(4), 742–755.

42. Yao, M. F., Chen, Z., Zheng, Z. Q., Zhang, B., Xing, Y. (2006) *Study on the Controlling Strategies of Homogeneous Charge Compression Ignition Combustion with Fuel of Dimethyl Ether and Methanol.* Fuel, Vol. 85(14–15), 2046–2056.

43. Yao, M. F., Zheng Z. L., Liu, H. F. (2009) *Progress and Recent Trends in Homogeneous Charge Compression Ignition (HCCI) Engines.* Prog. Energ. Combust., Vol. 35(5), 398–437.

44. Zeldovich, Y. B. (1946) *The Oxidation of Nitrogen in Combustion Explosions.* Acta Physico-Chimica. U.S.S.R., Vol. 21(4), 577–628.

45. Zhao, R., Gao, D., Pan, X. X. et al. (2018) Theoretical Studies of Anharmonic Effect on the Main Reactions Involving in NO_2 in Fuel Burning. Chem Phys Lett., Vol. 703, 97–105.

TOPIC GRAPH

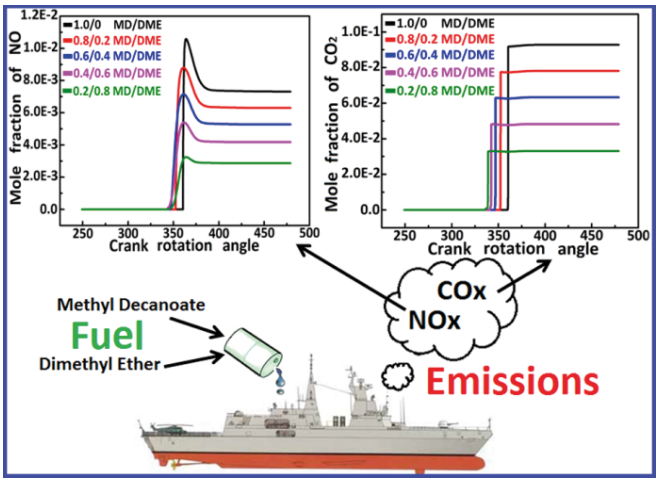

CONTACT WITH THE AUTHORS

Shiye Wang
e-mail: 675891906@qq.com

Marine Engineering College
Dalian Maritime University
Linghai, 116026 Dalian,
China

Li Yao
e-mail: yaoli@dicp.ac.cn

Merchant Marine College
Shanghai Maritime University
Pudong, 201306 Shanghai,
China